Master of science

Effect of frugoside on cell death in human melanoma cancer cells in vitro and in vivo

Frugoside 가 인간 흑색종 세포의 세포사멸에 미치는 영향

The Graduate School of University of Ulsan

Department of Medicine

Jimin Shin

Effect of frugoside on cell death in human melanoma cancer cells in vitro and in vivo

Supervisor : Sung-Wuk Jang

A Dissertation Submitted to the Graduated School of the University of Ulsan In Partial Fulfillment of the Requirements for the Degree of

Master of Science

by

Jimin Shin

Department of Medicine
Ulsan, Korea
February 2018

This certifies that the master thesis
of Jimin Shin is approved

_____

Commttee Vice-Chair Dr. Sun-cheol Choi

_____

Commttee Member Dr. Peter whan Lee

_____

Commttee Member Dr. Sung-wuk Jang

Department of Medicine
Ulsan, Korea
February 2018

Abstract

Malignant melanoma is the most life-threatening neoplasm of the skin, accounting for most of the skin cancer deaths. Its incidence is increasing worldwide and it is becoming resistant to current therapeutic agents. The bioactive compound frugoside, a new cardenolide glycoside from the leaves of *Calotropis procera* W.T. Aiton (family Asclepiadaceae), was recently reported to inhibit the growth of various human cancer cell lines *in vitro*. However, its modes of action on melanoma cancer have not been clearly defined. Here, I have shown that frugoside selectively inhibited the viability of human melanoma cancer M14 and A375 cells in a concentration- and time-dependent manner. Frugoside could significantly increase the generation of reactive oxygen species (ROS), which triggered the mitochondrial/caspase apoptotic pathway in M14 and A375 cells. The reducing of ROS generation with antioxidant N-acetyl-L-cystein and dipenyleneiodonium (DPI) conferred significant protection against frugoside-induced ROS generation, disruption of apoptotic mechanisms including loss of mitochondrial membrane potential, release of cytochrome-c, and activation of the caspase-cascade. Finally, frugoside exhibited a potential antitumor effect in M14 melanoma cancer xenografts without apparent toxicity. Taken together, the present study indicates that frugoside can induce melanoma cancer cell apoptosis and therefore represents therapeutic potential for cancer treatment.

Contents

List of Figures

Ⅰ. Introduction

Melanoma is one of the most aggressive forms of skin cancers with a high frequency of metastasis and with very poor prognosis in the metastatic stage [1, 2]. Although most patients with early-stage melanoma are cured with surgery alone, the majority of patients with metastatic disease will die of their disease soon after diagnosis. Even with recent therapeutic breakthroughs, the management of metastatic melanoma is very challenging, in part because there are few effective treatment modalities [3, 4, 5, 6, 7, 8]. Nevertheless, no agents have shown statistically significant improvement with a good prognosis in the treatment of malignant melanoma. Thus, discovery of more effective drugs with less toxicity are urgently needed.

The bioactive compound frugoside, a new cardenolide glycoside from the leaves of *Calotropis procera* W.T. Aiton (family Asclepiadaceae), was recently reported to inhibit the growth of various human cancer cells, including non-small cell lung cancer, glioblastoma, prostate cancer cell lines [9]. However, there are few information in the literature about the potential anti-cancer activity of frugoside.

Apoptosis is a programmed cell death with an energy-dependent mechanism. This phenomenon causes rapid destruction of cell structures and cell organelles [10, 11]. One of several signaling pathways that control apoptosis is the mitochondrial pathway [12]. Mitochondria participate in cell death mechanisms through the release of apoptogenic

proteins into the cytosol and generation of excess reactive oxidative species (ROS). The mitochondrial respiratory chain is a major source of cellular ROS and therefore, represents a target for the effect of ROS production

Oxidative stress is involved in a number of physiological and pathological processes, including cancer, neurodegenerative diseases, and arteriosclerosis [12]. ROS are products of normal metabolism and xenobiotic exposure, and depending on their concentration. Accumulating evidence has suggested that cancer cells have higher ROS levels than normal cells and are more vulnerable when encountering further ROS insults induced by exogenous agents [13, 14]. Excessive ROS production exhibits anticancer effects by caspase-dependent or -independent activation through mitochondria-mediated intrinsic apoptotic pathway [13, 15, 16].

In this study, I investigated the inhibitory effects of frugoside on the growth of human melanoma cancer and explored its underlying molecular mechanisms for frugoside-induced apopotosis in vitro and in vivo.

Ⅱ. Material and Method

1. Cell Culture

Human melanoma M14, A375 cell lines were cultured in RPMI1640 with 10% heat inactivated Fetal Bovine Serum (FBS), and added 1% antibiotics (Penicillin and streptomycin). Cells were maintained in an incubator under 37℃ and 5% CO_2.

2. Cell Viability assay

The MTT assay was used determine the respective cytotoxic effects of frugoside on M14, A375 cell lines. Cells (1×10^4) were seeded in 96-well culture plates, and treated with various concentrations (0, 0.25, 0.5, 1 μg/ml) of frugoside after cultured for 24 h. after 12, 24, 36 or 48 h of treatment, MTT solution (10 μl/100 μl) was added to each well of plate and incubation for 1-2 h in a CO_2 incubator at 37℃. The absorbance of each well was measured at 450 nm with a reference wavelength of 600 nm

3. Flow Cytometry for detection of cell death

M14, A375 cells were detected by the Annexin V-FITC/PI double staining kit (BD bioscience, cat.556547). In brief, cells (3×10^5) seeded in the 6-well plates and then treated with different concentrations of frugoside for 24 h. Cells were washed once with phosphate-buffered saline (PBS), trypsinized and harvested by centrifugation at 1800 r.p.m. for 3 min.

Final cell pellets were stained with annexin V fluorescein isothiocyanate and PI for 25 min in the supplied incubation buffer, and PI- and/or annexin V-positive cells were analyzed by flow cytometry using FACS Canto.

4. Western blot

Cells were lysed in lysis buffer A [20 mM N-2-hydroxyethylpiperazine-N'-2-ethanesulfonic acid (pH 7.5), 150 mM NaCl, 1 mM ethylenediaminetetraacetic acid, 2 mM ethylene glycol tetraacetic acid, 1% Triton X-100, 10% glycerol and proteasecocktail I/II (Sigma)],and cellular debris was removed by centrifugation at 15,000 r.p.m. for 15 min. Proteins were separated by sodium dodecyl sulfate polyacrylamide gel electrophoresis, transferred onto nitrocellulose membranes, blocked with 5% skim milk in 0.01M Tris-buffered saline (TBS; pH 7.5) containing 0.5% Tween 20 and blotted with the appropriate primary antibodies. Membranes were then incubated with horseradish peroxidase-conjugated goat anti-rabbit-IgG or goat anti-mouse-IgG secondary antibodies for 1h at room temperature and detected by chemiluminescence (Amersham, Uppsala, Sweden).

5. Mitochondrial Membrane Potential Assessment by TMRE

Mitochondrial membrane potential ($\Delta\psi m$) was assessed by flow cytometry (FACSCalibur, BD) using tetramethylrhodamine ethyl ester (TMRE; Molecular Probes), a nontoxic

monovalent cation that reversibly accumulates in the mitochondrial lipid environment according to membrane potential with a Nernstian distribution. After frugoside treatments, cultured A375, M14 cells were resuspended in PBS and incubated with TMRE 200 nM for 30 minutes in the dark at 37°C. At the end of incubation, cells were resuspended in the flow analysis buffer (PBS 1×), and kept on ice until analysis.

6. ROS detection

For Mito-SOX (invitrogen) Red–based flow cytometric detection of mitochondrial superoxide, A375, M14 cells were treated with frugoside for 24 h, and performed to harvest. Cells were incubated with 1uM Mito-SOX Red superoxide indicator for 30 minutes in CO_2 incubatior at 37℃ and washed in PBS, before cells were analyzed on a FACSCalibur (BD).

7. Ca^{2+} determination with Rhod2-AM

To measure mitochondrial calcium levels, cells were treated with 5uM Rhod2-AM (Invitrogen) and incubated at 37℃ for 30 minutes. After staining, cells were washed with phosphate buffered saline (PBS) and analyzed with a dual laser FACSCalibur flow cytometer (BD)

8. Colony forming

For the experiments with soft agar, all wells were pre-coated with 0.5% agarose as the bottom layer whereas the top layer is consisted of 0.3% agarose and tumor cells. M14 cells were plated at a cell density of 2×10^5 cells/well onto 6-well culture dishes, and incubated with frugoside treatment for 2 weeks. Cells were stained crystal violet and were washed with phosphate buffered saline (PBS). The number of colonies consisting of >50 cells was counted using a microscope.

9. Xenograft assay

Six-week-old male BALB/c nude mice were used for *in vivo* animal experiments. The animals were housed in constant laboratory conditions of a 12-h light/dark cycle and specific pathogen-free conditions and fed with water and food ad libitum. For xenograft study, mice were inoculated subcutaneously into the right-back with 2×10^6 M14 cells in 50 μl PBS. The mice were randomly assigned into two groups of 5 each; one group received frugoside, the other group was used as the control that received same amount of PBS. The body weight and tumor volume [(major axis) × (minor axis)2 × 1/2] of every mouse were monitored biweekly after 2 weeks up to the end of the experiment (4 weeks).

Ⅲ. Result

1. ***Frugoside inhibits cell viability of melanoma cells***

Frugoside structures is depicted in Fig. 1A. This cardenolide glycoside is previously shown to have potent cytotoxic effects on some human cancer cell lines [9]. I first investigated the inhibitory effects of frugoside on the growth of human melanoma cancer cell line M14 and A375. As shown in Fig. 2A and B, inhibition of cell viability was observed in M14 and A375 cells in a concentration-and time-dependent manner after treatment with frugoside. Next, I used flow cytometry after staining with propidium iodide (PI) and annexin V (AV) to assess the induction of cell death by frugoside in M14 and A375 cells. Treatment of both cell lines with various concentration frugoside for 24 hours induced a significant decrease in viable (PI^{low}/AV^{low}) cells ($P<0.01$), and an increase in apoptotic (PI^{hgih}/AV^{high}) cells ($P<0.01$ Fig. 3A and B). Similarly, sub-G1 phase was observed after frugoside treatment in M14 and A375 cells (Fig. 4A and B). Collectively, these data demonstrate that the reduced viability of melanoma cancer cells are due to induction of apoptosis.

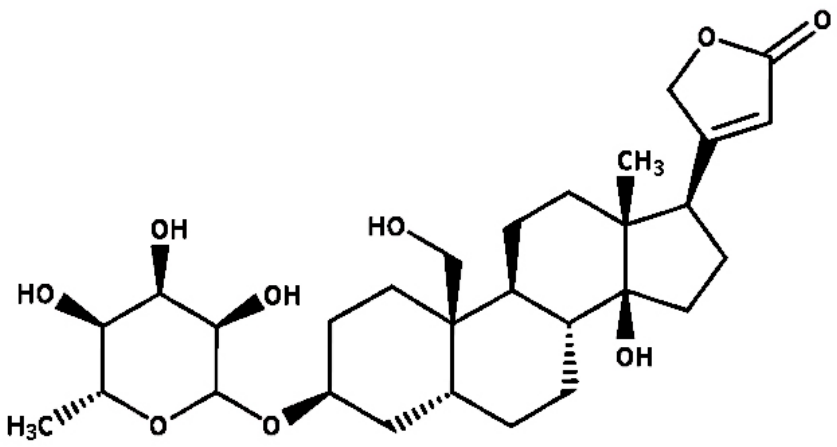

Fig. 1 Structure of frugoside

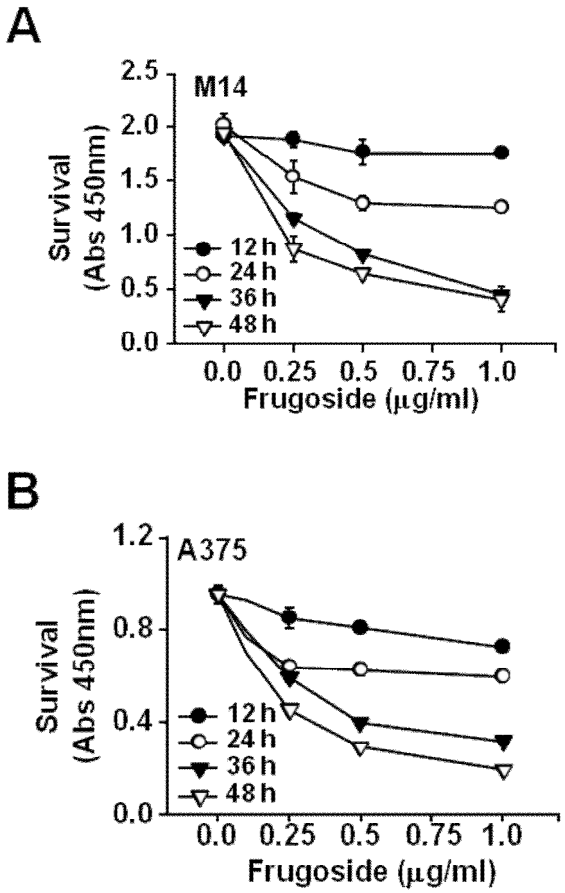

Fig. 2 Cell survival curve for cell viability in human melanoma cells.

(A) M14 cells were treated with different dose of frugoside (0, 0.25, 0.5, 1 ug/ml) for 12 h, 24 h, 36 h or 48 h and cell viability was measured by the MTT assay. (B) A375 cells were treated with different dose of frugoside (0, 0.25, 0.5, 1 ug/ml) for 12 h, 24 h, 36 h or 48 h and cell viability was measured by the MTT assay.

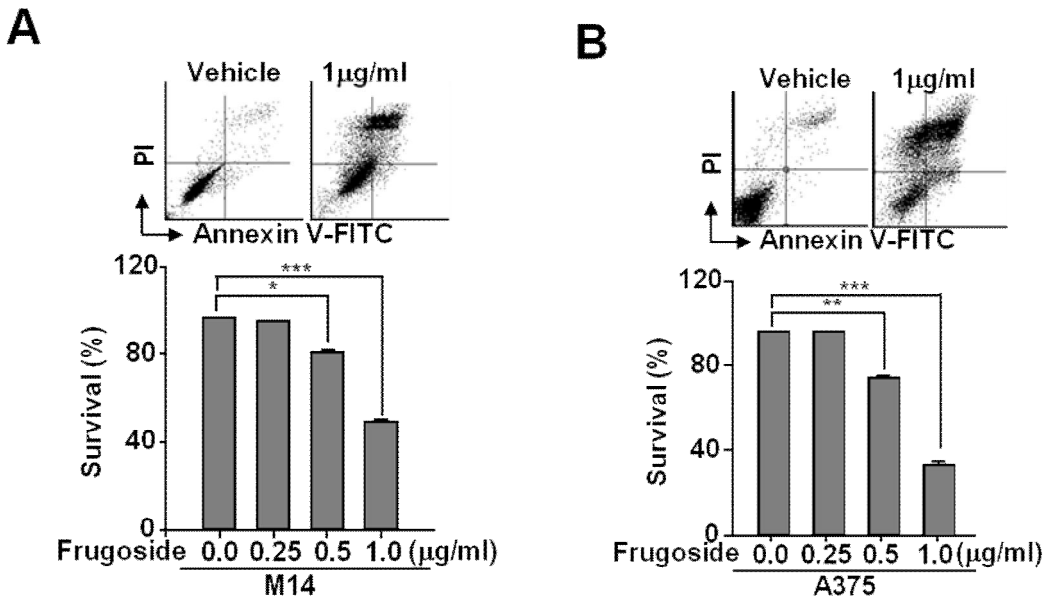

Fig. 3 Rate of apoptosis induced by fruoside in human melanoma cells

(A) Annexin-V/PI analysis by flow cytometry of M14 cells treated with different dose of frugoside (0, 0.25, 0.5, 1 ug/ml) for 24 h. (B) Annexin-V/PI analysis by flow cytometry of A375 cells treated with different dose of frugoside (0, 0.25, 0.5, 1 ug/ml) for 24 h.

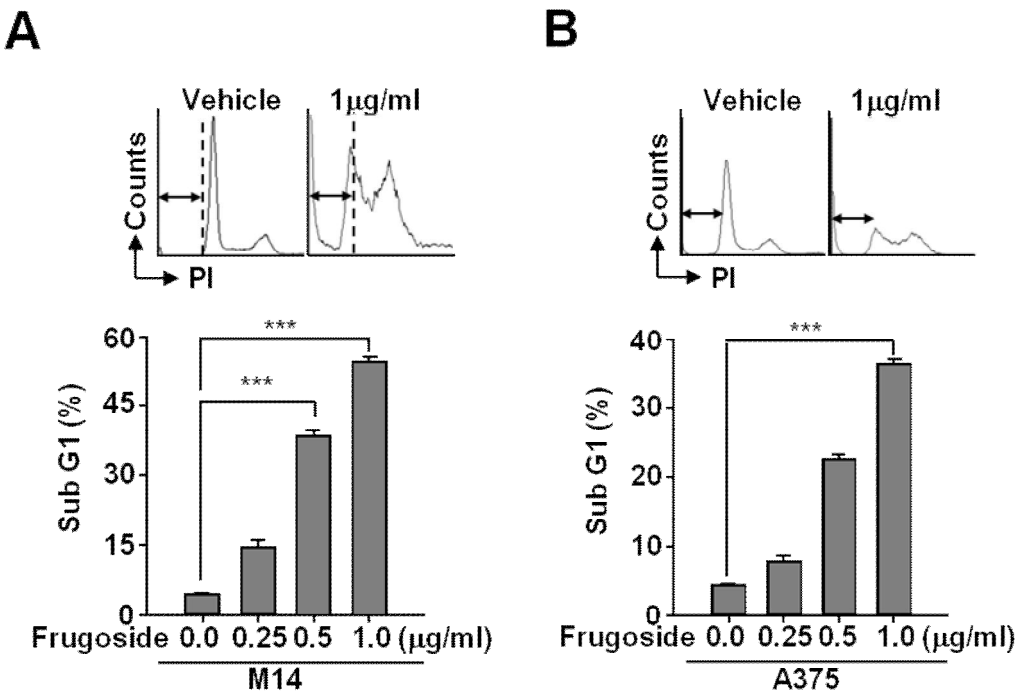

Fig. 4 DNA content (percent sub-G1) analysis of cells upon treatment with frugoside in human melanoma cells.

(A) Cell cycle analysis using propidium iodide (PI) staining and flow cytometry. M14 cells were treated with different dose of frugoside for 24 h. (B) Cell cycle analysis using propidium iodide (PI) staining and flow cytometry. A375 cells were treated with different dose of frugoside for 24 h.

2. ***Frugoside induces apoptosis through mitochondrial pathway.***

To confirm that apoptosis was induced by frugoside, western blotting was performed to detect cleavage of PARP, and caspase-3. Following frugoside treatment, cleavage of PARP and caspase-3 increased in a dose (Fig. 5A and B) and time dependent (Fig. 6A and B) manners in M14 and A375 cells. Cytochrome *c* release from mitochondria into cytosol is an upstream event in the activation of caspase cascade and a good measure of apoptotic processes. To examine the release of cytochrome *c* in frugoside treated M14 and A375 cells, we performed western blotting using cytosolic and mitochondrial fractions in M14 and A375 cells (Fig. 7A and B). My findings demonstrated that frugoside significantly induced the release of cytochrome *c* from the mitochondria into cytosol. To further investigate whether frguoside regulates mitochondrial activity, I examined the mitochondrial features of frugoside treated M14 and A375 cells in a dose and time dependent. Mitochondrial membrane potential ($\Delta\Psi m$) levels were lower in the frugoside-treated M14 and A375 cells compared to those in control cells (Fig. 8A and B). I next measured the mitochondrial ROS and Ca^{2+} levels by using Mito-Sox, an oxidant-sensitive fluorescent dye, and rhod2-AM, a

mitochondrial Ca^{2+}-sensitive dye, respectively. Frugoside treatment resulted in a remarkable increase in mitochondrial superoxide anion production (Fig. 9A and B) and in the Ca^{2+} levels (Fig. 10A and B). Interestingly, exposure to frugoside at a constant level (1 μg/ml) led to a time-dependent decrease in ΔΨm levels that was detected at 12 h (Fig. 8). However, ROS and Ca^{2+} levels were only detected at 24 h (Fig. 9 and 10). Taken together, our results suggest that the alterations in mitochondrial function caused by frugoside are involved in the susceptibility of melanoma cancer cells to frugoside-mediated cell death.

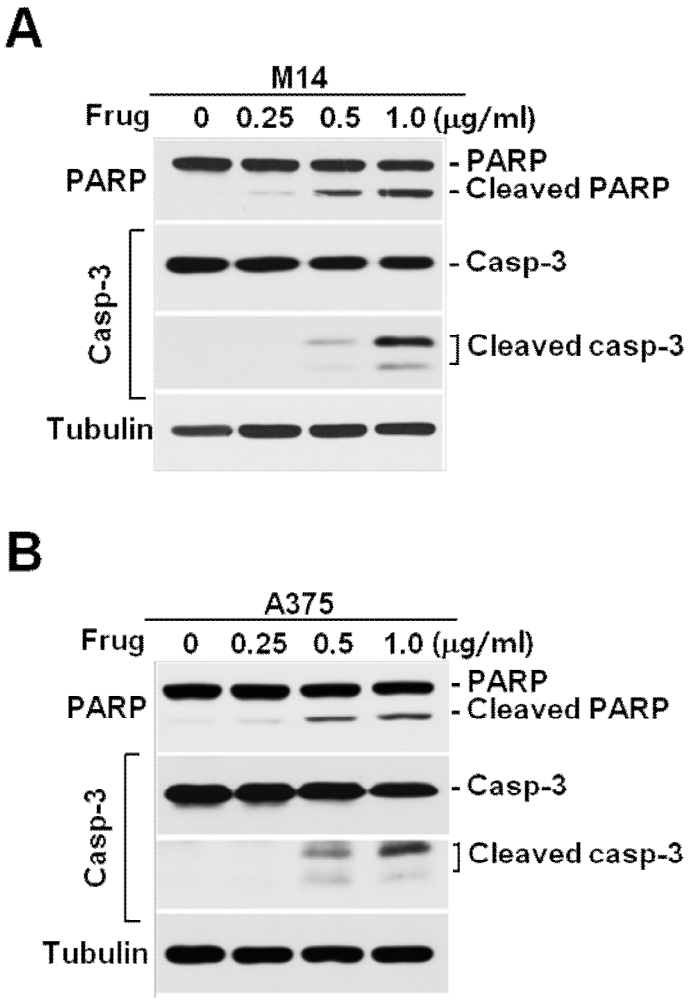

Fig. 5 Frugoside increases the cleavage of apoptosis related proteins in a dose - dependent manner.

(A) Western blot analysis for the expression of PARP, cleaved PARP, caspase-3 and cleaved caspase-3 in M14cells treated with different dose of frugoside (0, 0.25, 0.5,1 ug/ml) for 24 h. (B) Western blot analysis for the expression of PARP, cleaved PARP, caspase-3 and cleaved caspase-3 in A375 cells treated with different dose of frugoside (0, 0.25, 0.5,1 ug/ml) for 24 h.

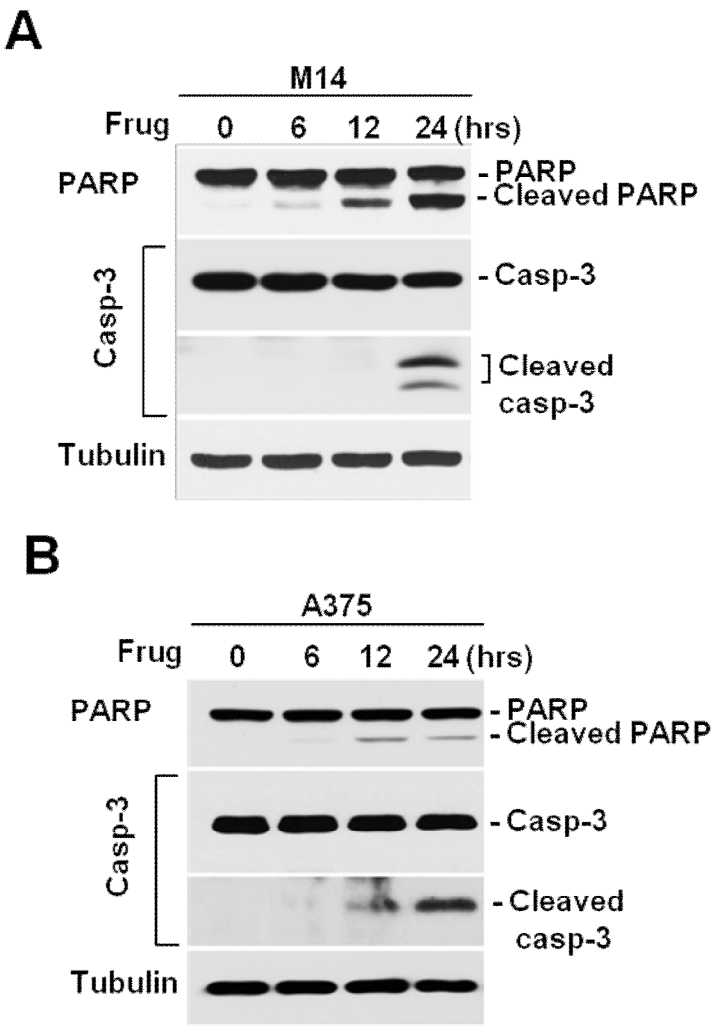

Fig. 6 Frugoside increases the cleavage of apoptosis-related proteins in a time-dependent manner..

(A) Western blot analysis for the expression of PARP, cleaved PARP, caspase-3 and cleaved caspase-3 in M14cells treated with frugoside (1 ug/ml) for 0 h, 6 h, 12 h and 24 h. (B) Western blot analysis for the expression of PARP, cleaved PARP, caspase-3 and cleaved caspase-3 in A375 cells treated with frugoside (1 ug/ml) for 0 h, 6 h, 12 h and 24 h.

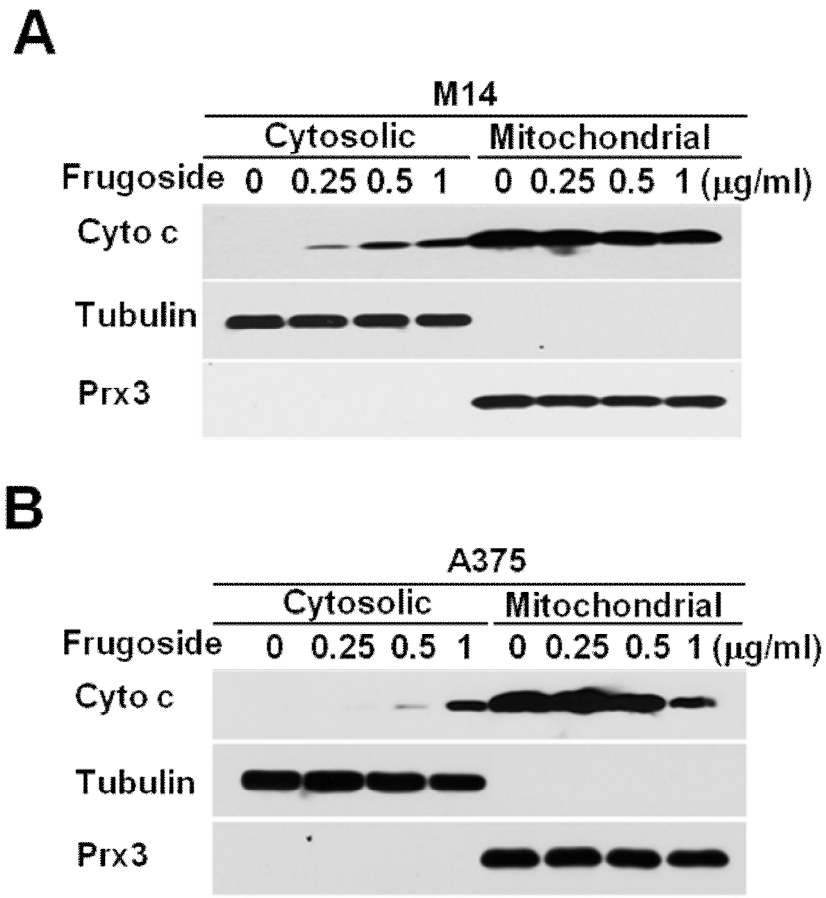

Fig. 7 Cytochrome c release by frugoside treatment in human melanoma cell.

(A) Western blot analysis of cytochrome c release in M14 cells treated with Frugoside (1 ug /ml) was performed in a dose dependent manner. (B) Western blot analysis of cytochrome c release in A375 cells treated with Frugoside (1 ug/ml) was performed in a dose dependent manner.

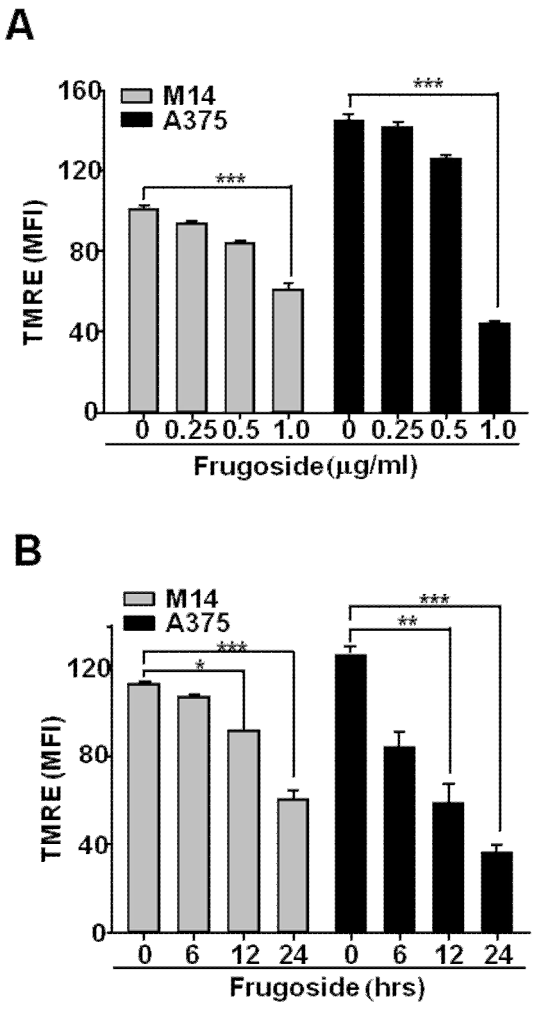

Fig. 8 Change of membrane potential by frusogide treatment

(A) Frugoside was treated in a dose - dependent manner for 24 h, followed by TMRE staining, followed by incubation for 30 minutes and FACS analysis. (B) Frugoside was treated in a time - dependent manner for 24 h, followed by TMRE staining, followed by incubation for 30 minutes and FACS analysis.

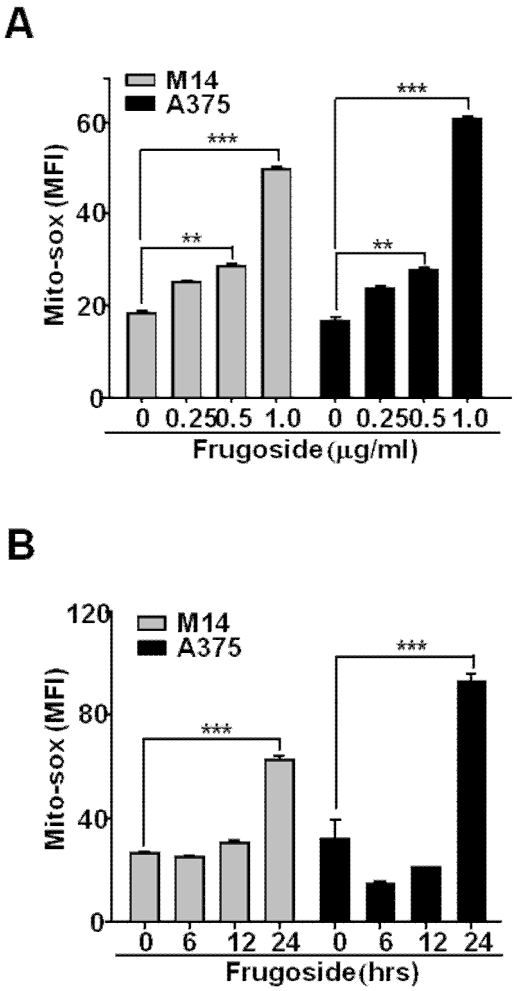

Fig. 9 Change of mitochondrial superoxide by frusogide treatment

(A) Frugoside was treated in a dose - dependent manner for 24 h, followed by Mito-sox staining, followed by incubation for 30 minutes and FACS analysis. (B) Frugoside was treated in a time - dependent manner for 24 h, followed by Mito-sox staining, followed by incubation for 30 minutes and FACS analysis.

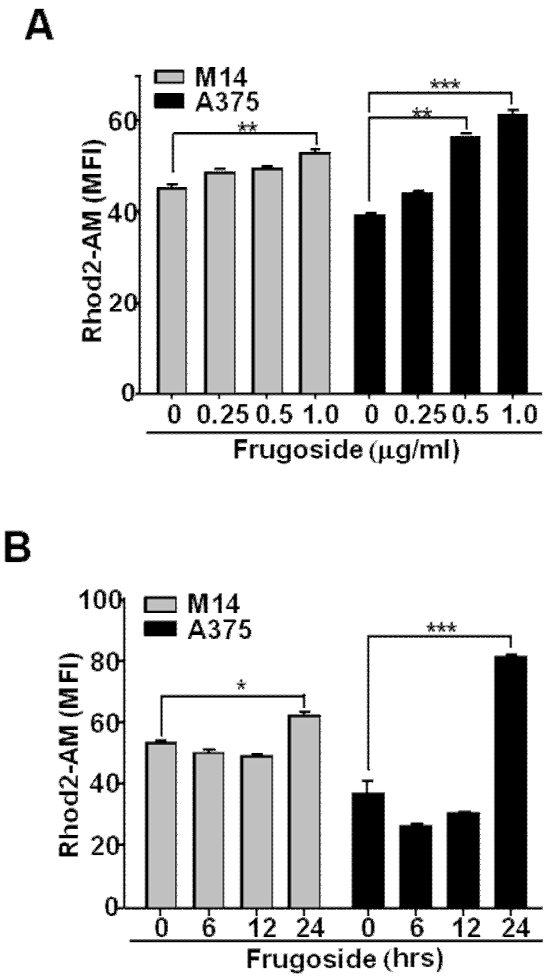

Fig. 10 Change of mitochondrial calcium overload by frusogide treatment

(A) Frugoside was treated in a dose - dependent manner for 24 h, followed by Rhod2-AM staining, followed by incubation for 30 minutes and FACS analysis. (B) Frugoside was treated in a time - dependent manner for 24 h, followed by Rhod2-AM staining, followed by incubation for 30 minutes and FACS analysis.

3. Oxidative stress was involved in frugoside-induced apoptosis

To determine whether the frugoside-induced apoptosis in melanoma cancer cells is mediated by elevated ROS level, I examined apoptosis induced by frugoside in cells pretreated with ROS scavenger N-acetyl cytein (NAC) or NOX inhibitor diphenyleneiodonium chlorid (DPI) for 24 h followed by PI and annexin V staining. As shown in Fig. 11A and B, NAC and DPI significantly inhibited the apoptotic effect of frugoside in M14 and A375 cells. Furthermore, western blot analysis indicated that treatment with NAC or DPI abrogated frugoside-mediated PARP and caspase 3 cleavage (Figure 12). These data indicated that ROS production is involved in frugoside-induced apoptosis.

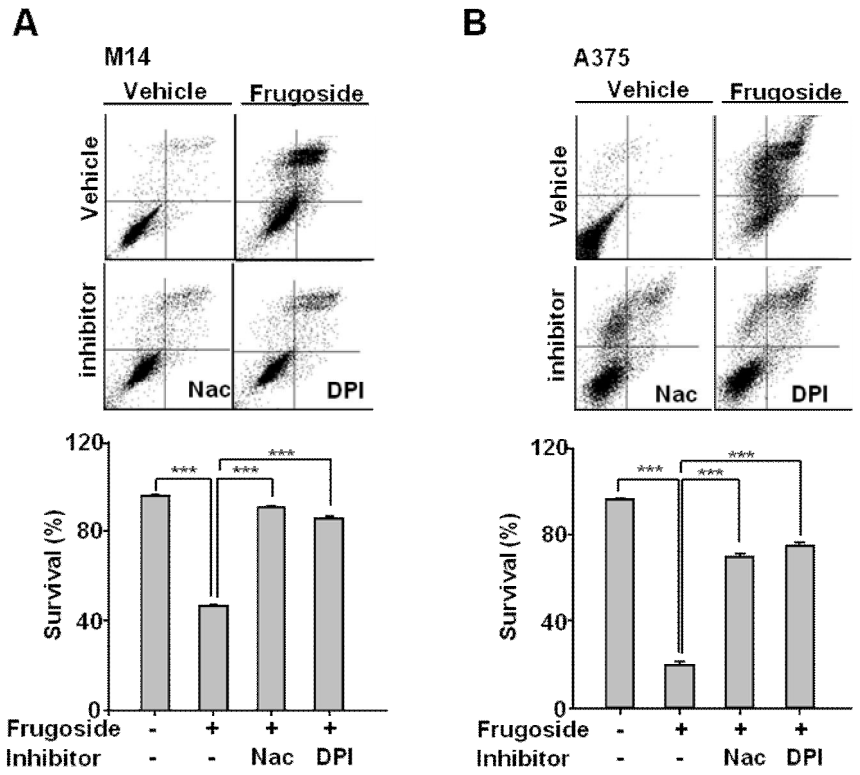

Fig. 11 Inhibition effect of NAC and DPI on frugoside in human melanoma cells

(A) NAC (60 Mm) and DPI (10 uM) are pretreated for 1 h, treated with frugoside in M14, and cultured for 24 h. Then, after the Annexin v-PI staining, perform FACS analysis. (B) NAC and DPI are pretreated for 1 h, treated with frugoside in A375, and cultured for 24 h. Then, after the Annexin v-PI staining, perform FACS analysis.

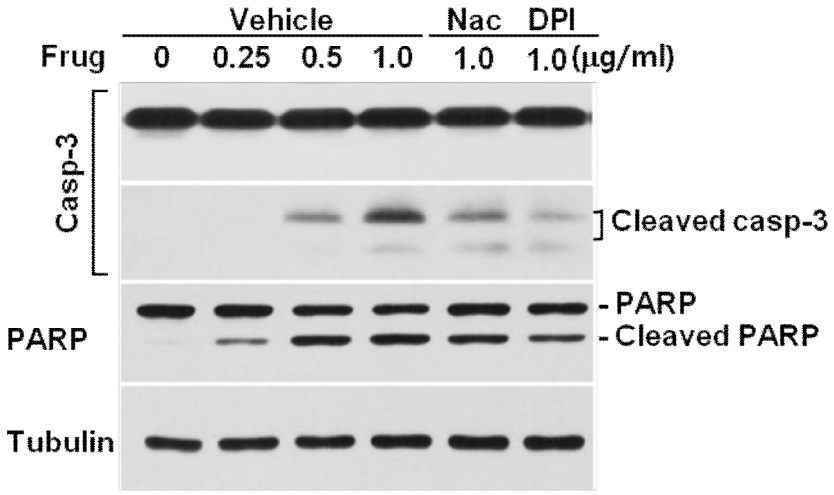

Fig. 12 NAC and DPI inhibit the cleavage of apoptosis-related protein by frugoside.

M14 cell is pretreated in NAC (60 mM) and DPI (10 μM) for 1 h and treated in frugoside. And then cleavage of apoptosis-related protein is confirmed by western blot.

4. ***Frugoside inhibits anchorage-independent growth and tumorigenicity***

Next, I evaluated the colony forming ability using the plate colony forming assay. The result showed that the frugoside treated M14 cells significantly decreased the colony forming rates compared the vehicle treated M14 cells (Fig. 13). Because frugoside suppresses anchorage-independent growth, I next examined the impact of frugoside on tumor promotion using a xenograft model in which M14 cells were subcutaneously injected under the flank of nude mice. As shown Fig. 14A, frugoside potently inhibited tumor growth as compared with control group. The avergage weight of tumors from frugoside treated mice was also significantly lower than that from the control mice (Fig. 14B). Moreover, no significant changes in body weight or adverse effect were observed in Frugosdie-treated mice (Fig. 14C).

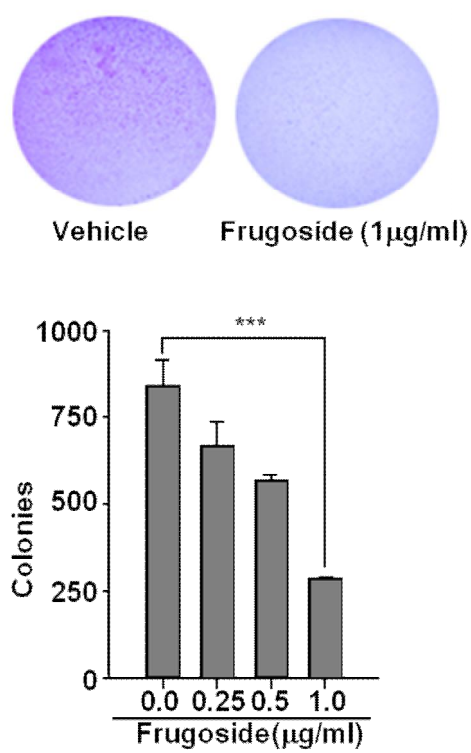

Fig. 13 The colony formation of M14 cells was repressed by frugoside treatment.

M14 cells were seeded in 6-well plates and cultured for 2 weeks at 37°C, 5% CO_2. After staining with crystal violet, we calculated the number of colonies formed. The results showed that in M14 cells, the number of clones formed by vehicles were more than those formed by frugoside treated cells

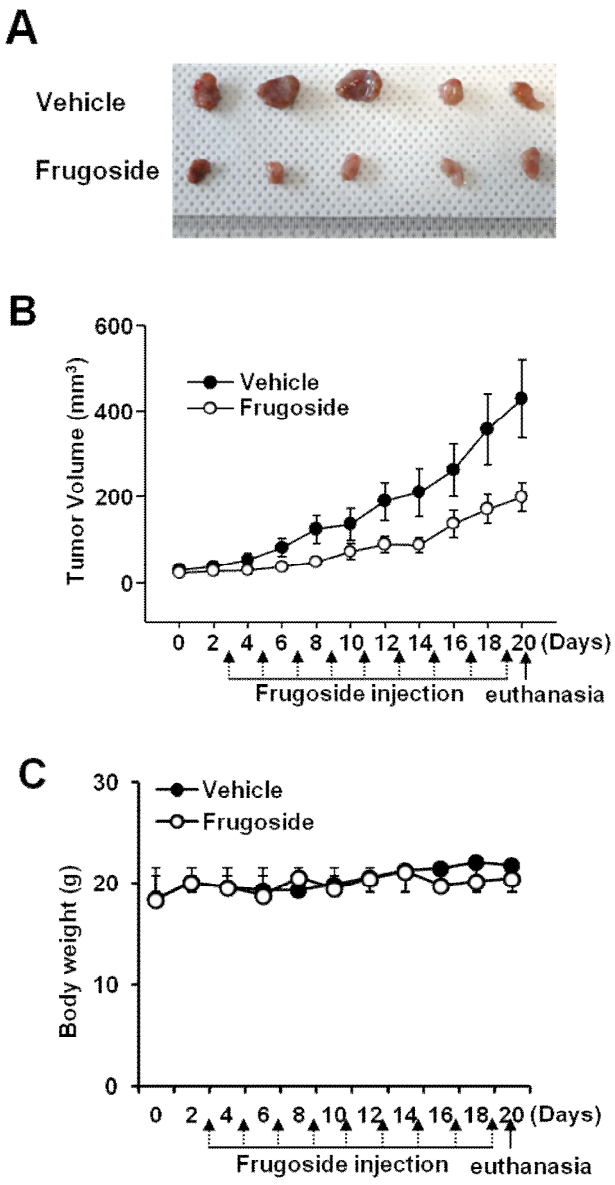

Fig. 14 Effects of frugoside on the growth of M14 tumors in *in vivo* xenograft models.

(A) Picture of changes in mouse tumor following frugoside injection. (B) Changes in the tumor volume following frugoside injection in two tumor models. Tumor volume at about 3 weeks following frugoside injection. (C) Animal weight treated with frugoside or control (n=5 mice/group, mean ± SD).

Ⅳ. Discussion

Melanoma is the most malignant form of skin cancer and is associated with a high mortality rate [17]. Current treatment modalities for melanoma include surgery, radiotherapy, chemotherapy, immunotherapy, and the use of biological agents. However, long-term survival chances for patients with melanoma remains poor even after aggressive treatment [18].

In recent years, various bioactive compounds derived from natural sources have been found to possess anticancer activities. Frugoside, a natural product of several medicinal plant, potently inhibits various cancer cell proliferation [9]. However, the molecular mechanisms underlying the anti-melanoma property of frugoside have not been investigated. The present study was conducted to elucidate the molecular basis for the frugoside-induced apoptosis in the melanoma cell model. I demonstrated that: (a) frugoside inhibits cell viability of melanoma cancer cells, (b) frugoside regulates mitochondrial function, (c) frugoside induces ROS generation, (d) consequently, frugoside induces cell death in human melanoma cancer cells through ROS gerneration.

In the intrinsic pathway, cellular stress increases mitochondrial membrane permeability, followed by cytochrome c release, apoptosome formation with Aparf-1, and caspase activation [19, 20]. Many studies have demonstrated that ROS plays a central role in the induction of apoptosis via a variety of mechanism, such as increased mitochondrial permeability, opening of transition pores, release of pro-apoptotic factors, and activation of cspase-9 by various anti-cancer agents. [21, 22, 23, 24, 25]. However, the molecular mechanism of frugoside-induced ROS production is not well understood. In the present study, I observed that frugoside induced cellular and mitochondrial ROS production in M14 and A375 cells, which could be attenuated by pre-treating the cells with NAC or DPI. These findings indicated that the generation of ROS from mitochondria was a key event in mediating the apoptotic effects of frugoside in the M14 melanoma cells.

When the increase of ROS reaches a threshold level, it triggers the opening of transition pores, which would lead to the decrease of $\Delta\Psi m$ and induce the side leakage of electrons from complex I, II, and III of the electron transport chain leading to rapid reaction with molecular oxygen to yield superoxide anion [26]. Moreover, mitochondrial ROS regulate

Ca^{2+} channels and stimulate a specific Ca^{2+} release, thereby contributing to the maintenance of cellular Ca^{2+} homeostasis [27]. Excessive Ca^{2+} load to the mitochondria may also induce ROS production and apoptosis by stimulating the release of apoptosis-promoting factors from the mitochondrial intermembrane space to the cytoplasm [28]. In the current work, frugoside-treated M14 and A375 cells showed an early increase in cellular ROS production and Ca^{2+} overloads before apoptosis, indicating that mitochondrial damage is possibly related to Ca^{2+} release caused by oxidative stress.

Based on the *in vitro* results, I sought to confirm the inhibitory effect of frugoside against melanoma growth using an *in vivo* tumor xenograft model in nude mice. Consistent with the in vitro studies, I found that frugoside significantly attenuated tumor growth without any apparent sign of toxicity in M14 cell xenografts, reduced tumor volume at different times of treatment, and decreased the average tumor weight at the end of the treatment.

In summary, my results indicate that frugoside inhibits cell proliferation, and induces apoptosis in the human melanoma M14 and A375 cells through ROS generation and intrinsic apoptotic pathway. Additionally, my results also indicate that frugoside attenuates tumor

growth in the M14 cell xenograft model of nude mice, and displays a strong anti-tumor activity. Therefore, these finding suggest that frugoside has the potential to be developed as a new agent for melanoma treatment.

Ⅴ. References

1. Su, W. C., Lin, Y. F., Yu, X. P., Wang, Y. X., Lin, X. D., Su, Q. Z., Shen, D. Y., and Chen, Q. X. (2017) Mitochondria-Associated Apoptosis in Human Melanoma Cells Induced by Cardanol Monoene from Cashew Nut Shell Liquid. *J Agric Food Chem* **65**, 5620-5631

2. Ye, T., Zhu, S., Zhu, Y., Feng, Q., He, B., Xiong, Y., Zhao, L., Zhang, Y., Yu, L., and Yang, L. (2016) Cryptotanshinone induces melanoma cancer cells apoptosis via ROS-mitochondrial apoptotic pathway and impairs cell migration and invasion. *Biomed Pharmacother* **82**, 319-326

3. Chapman, P. B., Hauschild, A., Robert, C., Haanen, J. B., Ascierto, P., Larkin, J., Dummer, R., Garbe, C., Testori, A., Maio, M., Hogg, D., Lorigan, P., Lebbe, C., Jouary, T., Schadendorf, D., Ribas, A., O'Day, S. J., Sosman, J. A., Kirkwood, J. M., Eggermont, A. M., Dreno, B., Nolop, K., Li, J., Nelson, B., Hou, J., Lee, R. J., Flaherty, K. T., McArthur, G. A., and Group, B.-S. (2011) Improved survival with vemurafenib in melanoma with BRAF V600E mutation. *N Engl J Med* **364**, 2507-2516

4. Balch, C. M., Soong, S. J., Gershenwald, J. E., Thompson, J. F., Reintgen, D. S., Cascinelli, N., Urist, M., McMasters, K. M., Ross, M. I., Kirkwood, J. M., Atkins, M. B., Thompson, J. A., Coit, D. G., Byrd, D., Desmond, R., Zhang, Y., Liu, P. Y.,

Lyman, G. H., and Morabito, A. (2001) Prognostic factors analysis of 17,600 melanoma patients: validation of the American Joint Committee on Cancer melanoma staging system. *J Clin Oncol* **19**, 3622-3634

5. Bastiaannet, E., Beukema, J. C., and Hoekstra, H. J. (2005) Radiation therapy following lymph node dissection in melanoma patients: treatment, outcome and complications. *Cancer Treat Rev* **31**, 18-26

6. Lee, C. W., Yen, F. L., Ko, H. H., Li, S. Y., Chiang, Y. C., Lee, M. H., Tsai, M. H., and Hsu, L. F. (2017) Cudraflavone C Induces Apoptosis of A375.S2 Melanoma Cells through Mitochondrial ROS Production and MAPK Activation. *Int J Mol Sci* **18**

7. Hassan, L., Pinon, A., Limami, Y., Seeman, J., Fidanzi-Dugas, C., Martin, F., Badran, B., Simon, A., and Liagre, B. (2016) Resistance to ursolic acid-induced apoptosis through involvement of melanogenesis and COX-2/PGE2 pathways in human M4Beu melanoma cancer cells. *Exp Cell Res* **345**, 60-69

8. Leung, A. M., Hari, D. M., and Morton, D. L. (2012) Surgery for distant melanoma metastasis. *Cancer J* **18**, 176-184

9. Gurung, A. B., Ali, M. A., Bhattacharjee, A., AbulFarah, M., Al-Hemaid, F., Abou-Tarboush, F. M., Al-Anazi, K. M., Al-Anazi, F. S., and Lee, J. (2016) Molecular docking of the anticancer bioactive compound proceraside with macromolecules involved in the cell cycle and DNA replication. *Genet Mol Res* **15**

10. Zhao, Y., Guo, C., Wang, L., Wang, S., Li, X., Jiang, B., Wu, N., Guo, S., Zhang, R., Liu, K., and Shi, D. (2017) A novel fluorinated thiosemicarbazone derivative- 2-(3,4-difluorobenzylidene) hydrazinecarbothioamide induces apoptosis in human A549 lung cancer cells via ROS-mediated mitochondria-dependent pathway. *Biochem Biophys Res Commun* **491**, 65-71

11. Arihara, Y., Takada, K., Kamihara, Y., Hayasaka, N., Nakamura, H., Murase, K., Ikeda, H., Iyama, S., Sato, T., Miyanishi, K., Kobune, M., and Kato, J. (2017) Small molecule CP-31398 induces reactive oxygen species-dependent apoptosis in human multiple myeloma. *Oncotarget* **8**, 65889-65899

12. Zhong, Y., Jin, C., Gan, J., Wang, X., Shi, Z., Xia, X., and Peng, X. (2017) Apigenin attenuates patulin-induced apoptosis in HEK293 cells by modulating ROS-mediated mitochondrial dysfunction and caspase signal pathway. *Toxicon* **137**, 106-113

13. Nabatchian, F., Moradi, A., Aghaei, M., Ghanadian, M., Jafari, S. M., and Tabesh, S. (2017) New 6(17)-epoxylathyrane diterpene: aellinane from Euphorbia aellenii induces apoptosis via mitochondrial pathway in ovarian cancer cell line. *Toxicol Mech Methods* **27**, 622-630

14. Ahn, J., Chung, Y. W., Park, J. B., and Yang, K. M. (2018) omega-hydroxyundec-9-enoic acid induces apoptosis by ROS mediated JNK and p38 phosphorylation in breast cancer cell lines. *J Cell Biochem* **119**, 998-1007

15. Kwon, S. J., Lee, J. H., Moon, K. D., Jeong, I. Y., Ahn, D. U., Lee, M. K., and Seo,

K. I. (2014) Induction of apoptosis by isoegomaketone from Perilla frutescens L. in B16 melanoma cells is mediated through ROS generation and mitochondrial-dependent, -independent pathway. *Food Chem Toxicol* **65**, 97-104

16. Diwakarla, S., Nagley, P., Hughes, M. L., Chen, B., and Beart, P. M. (2009) Differential insult-dependent recruitment of the intrinsic mitochondrial pathway during neuronal programmed cell death. *Cell Mol Life Sci* **66**, 156-172

17. Tse, A. K., Cao, H. H., Cheng, C. Y., Kwan, H. Y., Yu, H., Fong, W. F., and Yu, Z. L. (2014) Indomethacin sensitizes TRAIL-resistant melanoma cells to TRAIL-induced apoptosis through ROS-mediated upregulation of death receptor 5 and downregulation of survivin. *J Invest Dermatol* **134**, 1397-1407

18. Farias, C. F., Massaoka, M. H., Girola, N., Azevedo, R. A., Ferreira, A. K., Jorge, S. D., Tavares, L. C., Figueiredo, C. R., and Travassos, L. R. (2015) Benzofuroxan derivatives N-Br and N-I induce intrinsic apoptosis in melanoma cells by regulating AKT/BIM signaling and display anti metastatic activity in vivo. *BMC Cancer* **15**, 807

19. Green, D. R., and Reed, J. C. (1998) Mitochondria and apoptosis. *Science* **281**, 1309-1312

20. Ko, C. H., Shen, S. C., Yang, L. Y., Lin, C. W., and Chen, Y. C. (2007) Gossypol reduction of tumor growth through ROS-dependent mitochondria pathway in human colorectal carcinoma cells. *Int J Cancer* **121**, 1670-1679

21. Wu, C. C., and Bratton, S. B. (2013) Regulation of the intrinsic apoptosis pathway by reactive oxygen species. *Antioxid Redox Signal* **19**, 546-558

22. Yu, Y., Fan, S. M., Song, J. K., Tashiro, S., Onodera, S., and Ikejima, T. (2012) Hydroxyl radical (.OH) played a pivotal role in oridonin-induced apoptosis and autophagy in human epidermoid carcinoma A431 cells. *Biol Pharm Bull* **35**, 2148-2159

23. Haga, N., Fujita, N., and Tsuruo, T. (2005) Involvement of mitochondrial aggregation in arsenic trioxide (As2O3)-induced apoptosis in human glioblastoma cells. *Cancer Sci* **96**, 825-833

24. Jo, G. H., Kim, G. Y., Kim, W. J., Park, K. Y., and Choi, Y. H. (2014) Sulforaphane induces apoptosis in T24 human urinary bladder cancer cells through a reactive oxygen species-mediated mitochondrial pathway: the involvement of endoplasmic reticulum stress and the Nrf2 signaling pathway. *Int J Oncol* **45**, 1497-1506

25. Kello, M., Drutovic, D., Chripkova, M., Pilatova, M., Budovska, M., Kulikova, L., Urdzik, P., and Mojzis, J. (2014) ROS-dependent antiproliferative effect of brassinin derivative homobrassinin in human colorectal cancer Caco2 cells. *Molecules* **19**, 10877-10897

26. Cotgreave, I. A., and Gerdes, R. G. (1998) Recent trends in glutathione biochemistry--glutathione-protein interactions: a molecular link between oxidative stress and cell proliferation? *Biochem Biophys Res Commun* **242**, 1-9

27. Feissner, R. F., Skalska, J., Gaum, W. E., and Sheu, S. S. (2009) Crosstalk signaling between mitochondrial Ca2+ and ROS. *Front Biosci (Landmark Ed)* **14**, 1197-1218

VI. 국문요약(Summary in Korea)

악성 흑색종은 대부분의 피부암 사망 원인을 차지하며, 가장 위험한 악성 피부 종양으로 알려져 있다. 전 세계적으로 악성 흑색종은 증가하고 있는 추세를 보이고 있으며 지금까지 알려진 치료제에 대해 내성을 갖고 있다. Calotropis procera W.T. Aiton (Asclepiadaceae)의 잎에 많이 포함되어 있는 frugoside는 강심성 배당체 구조로 이루어진 생체 활성 화합물로써 최근 시험관 내에서 다양한 암세포주의 성장을 억제한다는 보고가 있다. 그러나 흑색종에서는 항암 효과 및 명확한 작용 기전은 밝혀지지 않고 있다. 본 논문에서는, frugoside를 이용하여 인간 흑색종 세포주인 M14와 A375의 생존력을 농도 및 시간 의존적으로 억제한다는 것을 확인하였다. 또한, frugoside가 M14와 A375 세포주에서 활성 산소종 (ROS)를 생성시킴으로써 미토콘드리아/카스파제(caspase) 경로를 통한 세포사멸을 유도한다는 것을 확인하였으며, 이를 검증하기 위해 NADPH의 산화 효소인 NOX의 선택적 저해제인 diphenyleneiodonium (DPI)와 활성 산소종 포착제인 N-acetyl-L-cystein (NAC)을 처리 한 결과, frugoside에 의해 생성된 활성 산소종이 저해되고 이를 통해 미토콘드리아의 막 전위의 손실과 시토크롬-c의 방출을 억제함으로써 세포사멸이 억제됨을 확

인 할 수 있었다. 마지막으로, M14 흑색종 세포주를 이용한 이종 이식 동물 모델을 통하여 생체 내에서 frugoside의 효과를 검증하였다. 종합하면, 본 연구는 frugoside가 흑색종 세포에서 활성 산소종을 생성함으로써 세포 사멸을 유도 할 수 있고 이를 통하여 암 치료를 위한 치료적 가능성을 있다는 것을 확인하였다.